DOE/ET/53088-73 IFSR #73

DRIFT WAVES IN A STELLARATOR

A. Bhattacharjee,
J. E. Sedlak,
P. L. Similon,
M. N. Rosenbluth,
and D. W. Ross

Institute for Fusion Studies
The University of Texas at Austin
Austin, Texas 78712
November 1982

DRIFT WAVES IN A STELLARATOR

A. Bhattacharjee, J. E. Sedlak, P. L. Similon,
M. N. Rosenbluth, and D. W. Ross

Institute for Fusion Studies
The University of Texas at Austin
Austin, Texas 78712

Abstract

We investigate the eigenmode structure of drift waves in a straight stellarator using the ballooning mode formalism. The electrons are assumed to be adiabatic and the ions constitute a cold, magnetized fluid. The "effective potential" has an overall parabolic envelope but is modulated strongly by helical ripples along $\underset{\sim}{B}$. We have found two classes of solutions: those that are strongly localized in local helical wells, and those that are weakly localized and have broad spatial extent. The weakly localized modes decay spatially due to the existence of Mathieu resonances between the periods of the eigenfunction and the "effective potential."

In this Letter, we investigate the structure of drift eigenmodes in a straight stellarator. For a low-beta stellarator, such as Wendelstein VII-A, the equilibrium magnetic field $\underset{\sim}{B}$ is, in first approximation, the vacuum solution[1] which, in cylindrical geometry (r,θ,z) with one ignorable helical coordinate, is given by $B_r = \ell b I_\ell'(\ell\rho) \sin \ell u$, $B_\theta = \ell b/\rho \; I_\ell(\ell\rho) \cos \ell u$, $B_z = B_0 - \ell b I_\ell(\ell\rho) \cos \ell u$. The solutions depend

only on the dimensionless coordinates $\rho \equiv \alpha r$ and $u \equiv \theta - \alpha z$, where the pitch $\alpha \equiv n/\ell R$; n is the number of toroidal, ℓ the poloidal, field periods of the external helical coils, and $2\pi R$, the periodicity length of the cylinder. B_0 is a straight, uniform, axial magnetic field modulated by a helical field proportional to the parameter b. For $\ell = 2$ stellarators, the existence of nested magnetic surfaces requires $b/B_0 < 1$. The rotational transform for these fields is known[1] and occurs at second order in b/B_0. For Wendelstein VII-A [2], in which the fields have weak shear, $\iota \simeq 0.6$. This corresponds to $b/B_0 \simeq 0.58$ ($\ell = 2$, $n = 5$)

It will be convenient to represent the magnetic field $\underset{\sim}{B}$ in the Clebsch form $\underset{\sim}{B} = \underset{\sim}{\nabla}\Psi \times \underset{\sim}{\nabla}\beta$, where Ψ is the helical flux function, given by

$$\Psi = \frac{B_0 R^2}{2n/\ell}\left(\rho^2 - \frac{2b\rho}{B_0} I'_\ell \cos \ell u\right) , \qquad (1)$$

and β is an angle-like, multiple-valued function of position in a torus. Then

$$\underset{\sim}{\nabla}\beta = \frac{\underset{\sim}{B}\times\underset{\sim}{\nabla}\Psi}{|\underset{\sim}{\nabla}\Psi|^2} + \underset{\sim}{\nabla}\Psi\Lambda , \qquad (2)$$

where $\Lambda \equiv \underset{\sim}{\nabla}\Psi\cdot\underset{\sim}{\nabla}\beta/|\underset{\sim}{\nabla}\Psi|^2$, is proportional to the scalar component of $\underset{\sim}{\nabla}\beta$. In order to determine an equation for Λ, we take the curl of Eq. (2), and then its dot product with $\underset{\sim}{B}\times\underset{\sim}{\nabla}\Psi$. We get

$$\underset{\sim}{B}\cdot\underset{\sim}{\nabla}\Lambda \;=\; \frac{B^2}{|\underset{\sim}{\nabla}\Psi|^2}\,(\hat{b}\times\hat{\psi})\cdot\left[(\hat{b}\cdot\underset{\sim}{\nabla})\hat{\psi} - (\hat{\psi}\cdot\underset{\sim}{\nabla})\hat{b}\right] \quad , \tag{3}$$

where $\hat{b} \equiv \underset{\sim}{B}/B$ and $\hat{\psi} \equiv \underset{\sim}{\nabla}\Psi/|\underset{\sim}{\nabla}\Psi|$. By integrating Eq. (3) along the field line with the initial condition $\Lambda = 0$ at $s = 0$ [3] (s is the length along a field line), we may compute $\underset{\sim}{\nabla}\beta(s)$.

In Fig. 1, we show a plot of $|\underset{\sim}{\nabla}\beta|^2/|\underset{\sim}{\nabla}\beta|^2_{s=0}$ along a field line situated approximately half-way between the axis and the separatrix for $b/B_0 = 0.58$. The sharp contrast with the analogus cylindrical tokamak should be noted. Whereas, in a tokamak, $|\underset{\sim}{\nabla}\beta|^2$ is parabolic, in a straight stellarator, the overall parabolic envelope is modulated strongly by rapid helical ripples along $\underset{\sim}{B}$. This important distinction will lead to qualitatively different eigenmode structures in the stellarator problem.

In order to study drift-like eigenmodes in the geometry described above, we adopt a simple model in which the electron response is adiabatic, and the ions constitute a cold, magnetized fluid. The electrostatic eigenmode equation is derived from the quasi-neutrality condition. The derivation is standard, and we state the result

$$\left[\frac{c_s^2}{\omega^2}\nabla_\parallel^2 - \rho_s^2\nabla_\perp^2 - (\underset{\sim}{v}_* + \underset{\sim}{v}_d)\cdot\frac{\underset{\sim}{\nabla}_\perp}{i\omega} + 1\right]\frac{e\phi}{T_e} \;=\; 0 \quad . \tag{4}$$

Here, $c_s^2 \equiv T_e/m_i$, $\rho_s \equiv c_s/\Omega_i$, and the other symbols have the usual meanings. The diamagnetic drift is $\underset{\sim}{v}_* \equiv -(T_e/eB)n^{-1}(dn/d\Psi)\hat{b}\times\underset{\sim}{\nabla}\Psi$, and the magnetic drift $\underset{\sim}{v}_d \equiv 2T_e/eB\;\hat{b}\times\underset{\sim}{\kappa}$. The first term in Eq. (4) comes from the parallel motion of ions, the second from the polarization

drifts, the third from the diamagnetic and curvature drifts, and the last from the electron response.

Use of the ballooning mode formalism facilitates analysis of the eigenmode Eq. (4). Let us consider perturbations $e\phi/T_e = \tilde{\phi}(s)\exp(im\beta)$, with high wavenumber perpendicular to $\underset{\sim}{B}$ and varying slowly along $\underset{\sim}{B}$. Equation (4) reduces approximately to the one-dimensional form

$$\frac{c_s^2}{\omega^2}\frac{d^2\tilde{\phi}}{ds^2} = -\left[m^2|\underset{\sim}{\nabla}\beta|^2\rho_s^2 - \frac{(\underset{\sim}{v}_* + \underset{\sim}{v}_d)\cdot m\underset{\sim}{\nabla}\beta}{\omega} + 1\right]\tilde{\phi} \equiv Q\tilde{\phi} \qquad (5)$$

In order to obtain an appropriate dimensionless form of Eq. (5), we scale s to $k_0^{-1} \equiv 2\pi/\ell\alpha$, which is approximately the connection length, the frequency ω to the characteristic acoustic frequency $k_0 c_s$, and define a mode number parameter $\chi \equiv m\rho_s|\underset{\sim}{\nabla}\beta|_{s=0}$ (analogus to $k_\perp\rho_s$ at s = 0 in the tokamak literature).

The boundary condition as $|s| \to \infty$ is assumed to be of the WKB form, and we chose the branch which corresponds to waves with out-going energy. Since, by construction, the "effective potential" is symmetric about s = 0, the solutions must obey at s = 0 either $d\tilde{\phi}/ds = 0$ (even modes) or $\tilde{\phi} = 0$ (odd modes). In what follows, we have dealt exclusively with even modes which are well-known to be the least damped solutions.

Equation (5) has been solved numerically by shooting, using a sixth-order Numerov scheme. Details have been given elsewhere.[4] It should be emphasized here that the frequency spectrum is highly degenerate, and is often difficult to resolve numerically. For the cases cited below, $b/B_0 = 0.58$, the average radius of the flux surface

$r_0 \equiv \left(2\Psi/B_0\alpha\right)^{1/2} \simeq 0.1$ and the density scale-length parameter $L_n/R \equiv -\left(1/n\ dn/dr\right)^{-1}/R = 0.05$, which is approximately the same as the aspect ratio of Wendelstein VII-A.

We have found, consistent with the physical model, eigenmodes which are almost marginally stable, with a very small negative imaginary component in the eigenfrequency ω ($\equiv \omega_r + i\gamma$, $\gamma < 0$) . We classify them loosely under the two following categories:

(1) Strongly Localized Modes: In Fig. 2, we show a strongly localized solution for which $\chi = 0.8$. The eigenfunction decays rapidly, and is almost entirely contained in the first couple of helical wells. There is some amount of "tunnelling" of the eigenfunction between the first real turning point and the next, but "tunnelling" is negligible thereafter.

(2) Weakly Localized Modes: In Fig. 3, we show a weakly localized solution for which $\chi = 0.3$. The helical wells are too shallow to contain the eigenfunction, and there is considerable "tunnelling" between neighboring turning points. The spatial decay of the eigenfunction is actually due to a novel resonance between the period of the wave and that of the helical ripple. When the resonance condition is met, there is constructive interference between the wavelets reflected by the local barriers provided by the ripples, and the eigenfunction exhibits a sharp decay over the resonance region.

The nature of the resonance described above may be made somewhat more precise by modelling the resonance region approximately, using a Mathieu-like equation $d^2\tilde{\phi}/ds^2 + (a + q\ \cos\ 2s)\tilde{\phi} = 0$, where a and q are slowly varying functions of s . As is well-known[5], there are well-defined regions in (a,q) space, where the solution to Mathieu's

equation is either purely oscillatory ("stable") or decaying ("unstable"), and that the latter class of solution comes about when a satisfies certain resonance conditions. We have found that these conditions are indeed approximately satisfied by the effective potential when the eigenfunction enters the resonance region, and the spatial decay of the eigenfunction may then be estimated from the Mathieu exponents for "unstable" solutions. In Figs. 3(a) and 3(b) we have indicated the first resonance region. Subsequent resonance regions follow, and provide an effective mechanism for the spatial decay of the eigenfunction.

It is to be noted that in both the categories described above, the ion Landau resonance point may fall beyond the region in which the eigenfunction is localized, thus validating the fluid ion treatment. In particular, for the weakly localized solutions, what this means is that the ion resonance point may actually fall beyond the first Mathieu resonance. This raises the interesting possibility that not only the strongly localized mode, but also the weakly localized mode may be driven unstable by nonadiabaticity in the electron response caused, for example, by trapping in the helical wells.

To summarize, we have found almost marginally stable, drift-like eigenmodes in a straight stellarator. Unlike in a straight tokamak, in which the parabolic anti-well potential leads only to eigenmodes which are convectively damped by shear, the helical ripple and the short connection length in a straight stellarator allows for the existence to bound states, either by localization in neighboring helical wells, or by a resonance between the period of the eigenfunction and that of the helical ripples on an overall anti-well envelope. Inclusion of toroidal

effects may introduce, as in the toroidal tokamak problem, an additional branch in the dispersion equation.[6] The investigation of that, and nonadiabatic effects in the electron response, is left to future work.

This work is supported by United States Department of Energy contract number DE-FG05-80ET-53088.

References

1. A. I. Morosov and L. S. Solovév, Reviews of Plasma Physics (M. A. Leontovitch, ed.) 2, (Consultants Bureau, New York, 1966).
2. Wendelstein VII-A Group, 9th International Conference on Plasma Physics and Controlled Nuclear Fusion Research, (International Atomic Energy Agency, Baltimore, 1982), paper L-5.
3. This choice corresponds to $\eta_0 = 0$ in the tokamak literature. See, for example, R. J. Hastie, K. W. Hesketh, and J. B. Taylor, Nucl. Fusion 19, 1223 (1979). More generally, the local eigenvalue ω depends on $\Lambda(0) \equiv \Lambda_0$, but the choice $\Lambda_0 = 0$ is justified because it is a stationary point of $\omega(\Lambda_0,\Psi)$ by reason of symmetry.
4. N. T. Gladd and W. Horton, Jr., Phys. Fluids 16, 879 (1973).
5. See, for example, C. M. Bender and S. A. Orszag, Advanced Mathematical Methods for Scientists and Engineers, (McGraw-Hill, New York, 1978), pp. 560-566.
6. L. Chen and C. Z. Cheng, PPPL-1562 (Princeton Plasma Physics Laboratory, New Jersey, 1979).

Figure Captions

Fig. 1 $|\nabla\beta|^2/|\nabla\beta|^2_{s=0}$ along a field line on a surface passing through $r = 0.1$, $\theta = 0$, $z = 0$, for $b/B_0 = 0.58$.

Fig. 2 Strongly localized solution on the same surface as in Fig. 1. $\chi = 0.8$ and $L_n/R = 0.05$.

Fig. 3 Weakly localized solution on the same surface as in Fig. 2. $\chi = 0.3$ and $L_n/R = 0.05$.

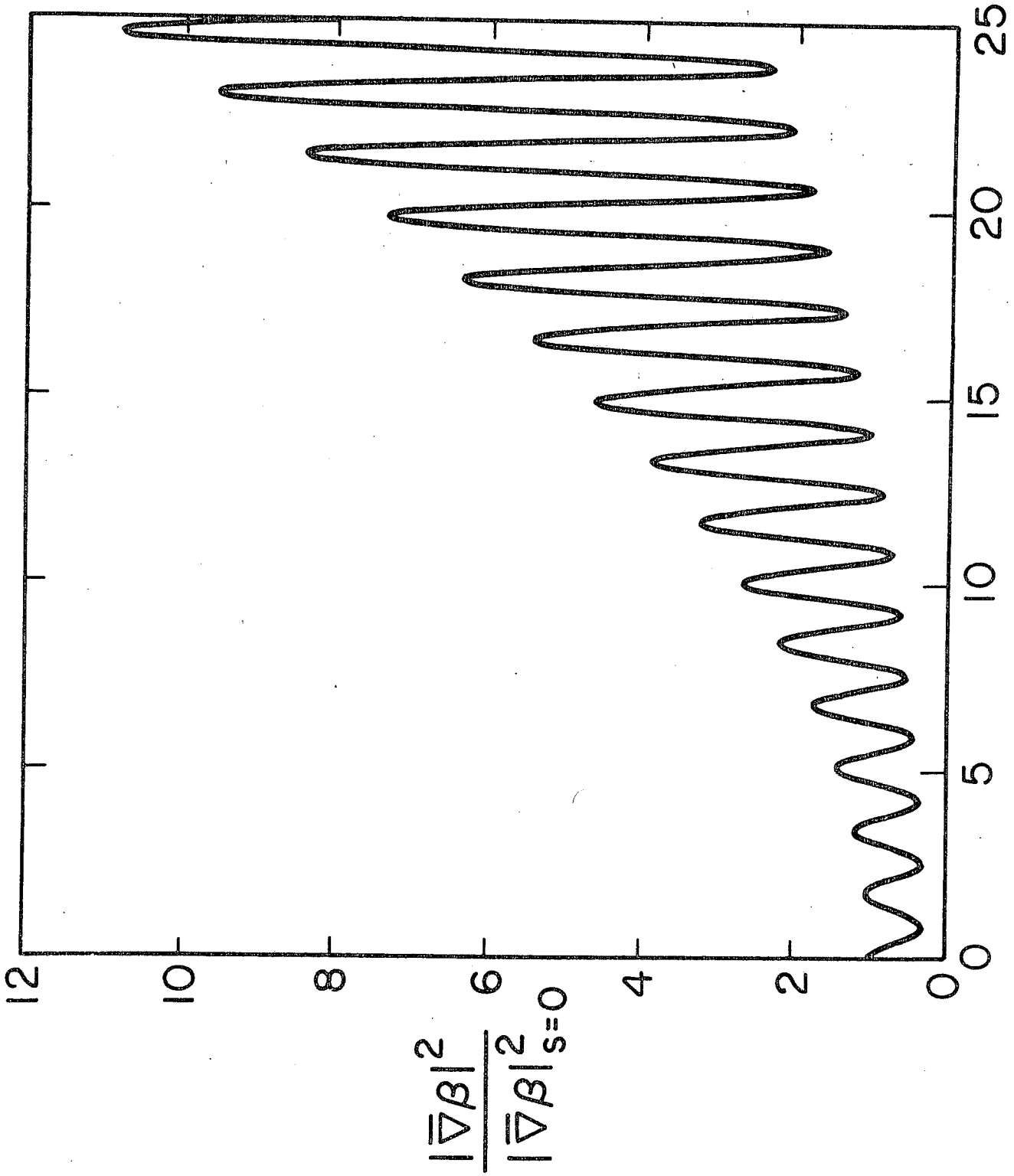

Fig. 1

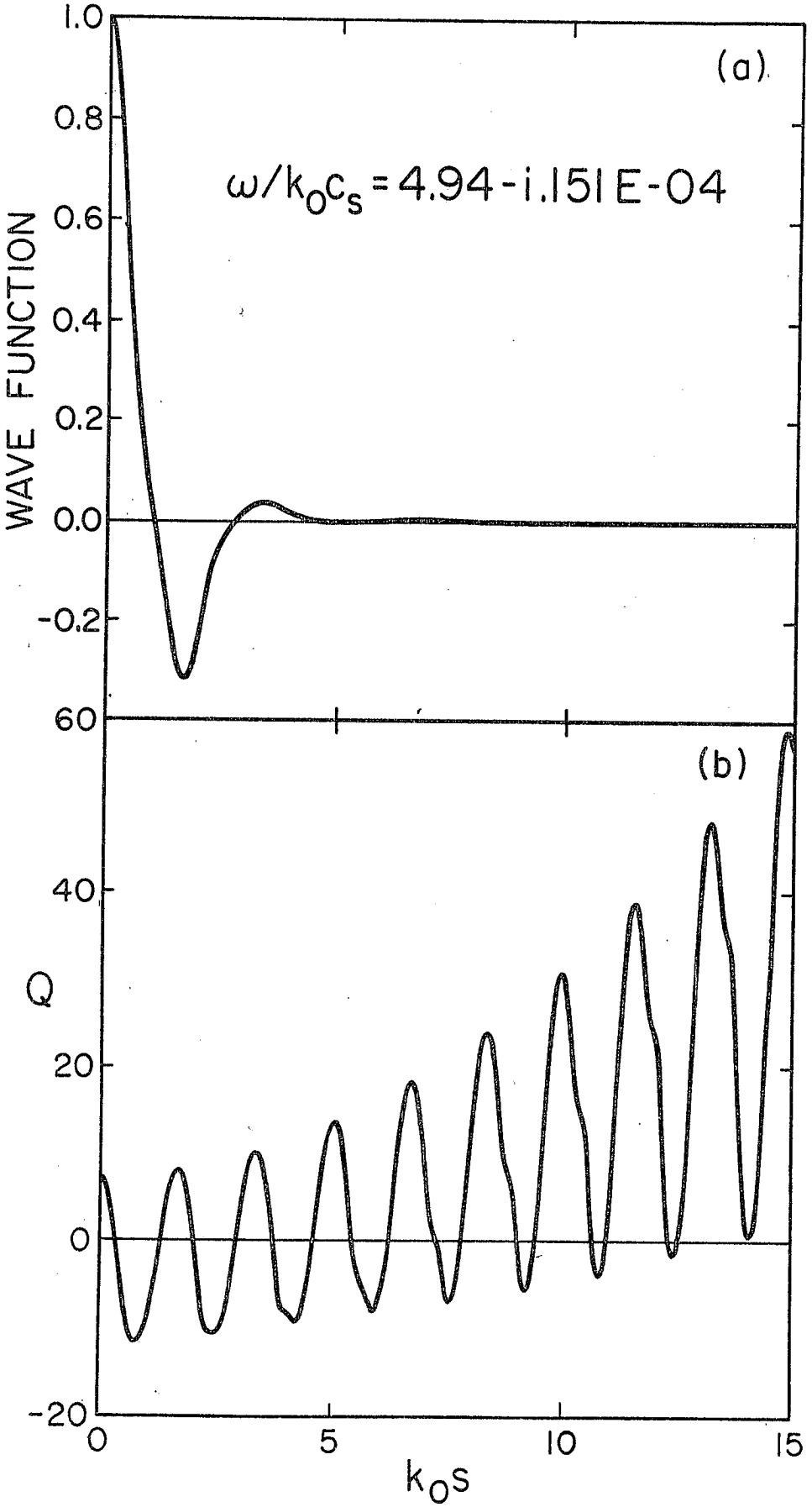
(a)
$\omega/k_0c_s = 4.94 - i.151E-04$
WAVE FUNCTION
1.0
0.8
0.6
0.4
0.2
0.0
-0.2
(b)
Q
60
40
20
0
-20
0
5
10
15
k_0s

Fig. 2

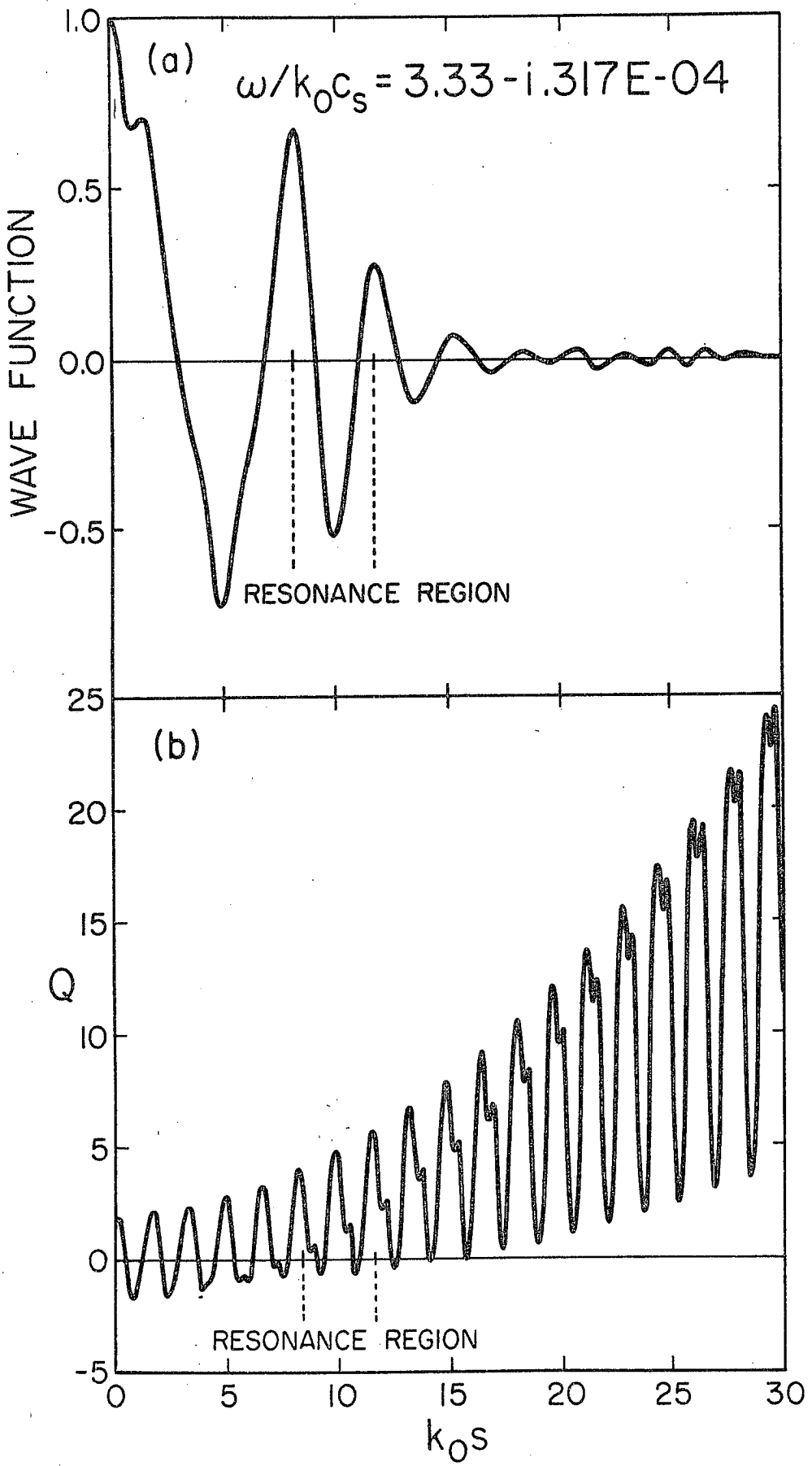
(a)
$\omega/k_0c_s = 3.33 - i.317E-04$
WAVE FUNCTION
1.0
0.5
0.0
-0.5
RESONANCE REGION
(b)
Q
25
20
15
10
5
0
-5
RESONANCE REGION
0
5
10
15
20
25
30
k_0s

Fig. 3